

**Title:**

Analysis of the physical stability of PCM slurries

**Authors:**

Mónica Delgado<sup>a,\*</sup>, Ana Lázaro<sup>a</sup>, Conchita Peñalosa<sup>a</sup>, Javier Mazo<sup>a</sup>, Belén Zalba<sup>a</sup>

<sup>a</sup>Aragón Institute for Engineering Research (I3A), Thermal Engineering and Energy Systems Group,  
University of Zaragoza

Agustín Betancourt Building, C/María de Luna 3, 50018 Zaragoza, Spain

\*Corresponding Author: [monica@unizar.es](mailto:monica@unizar.es); Phone: (+34) 976761000 ext: 5258; Fax: (+34) 976762616

## Abstract

Microencapsulated phase change material slurry (mPCM slurry) is a latent heat storage fluid in which the PCM microparticles have been dispersed in water. One of the main issues to be tackled is its lack of physical stability, since stratification problems tend to occur. Generally, an unstabilization process in PCM slurries can take weeks or even months. To predict the physical stability of PCM slurries without having to wait so long, a methodology well known in the food and pharmaceutical fields has been applied. This methodology basically consists of measuring samples with a rheometer in oscillatory mode. These measurements can be related to visually obtained measurements of the unstabilization process of creaming, specifically with the creaming percentage over time. From the frequency sweeps accomplished, an exponential relationship between the creaming percentage and the elastic module of the PCM slurries have been obtained. From the strain sweeps, the cohesive energies of the PCM slurries have been calculated and related to the creaming percentage, observing a linear relationship. In this way, the dominant parameters in the unstabilization process have been obtained which manufacturers can modify in order to improve the physical stability of PCM slurries.

## Keywords

PCM slurries; Phase Change Materials; Physical stability; Rheology

## Nomenclature

|       |                                      |
|-------|--------------------------------------|
| $E_c$ | cohesive energy ( $J \cdot m^{-3}$ ) |
| $G'$  | elastic modulus (Pa)                 |
| $G''$ | viscous modulus (Pa)                 |
| $k$   | fitting coefficient (s)              |
| $m$   | fitting coefficient (-)              |
| $t$   | time (s)                             |
| $V$   | volume ( $m^3$ )                     |

## Subscripts

|          |                     |
|----------|---------------------|
| $CR$     | critical strain     |
| $0$      | at low shear rates  |
| $\infty$ | at high shear rates |

## Greek symbols

|          |            |
|----------|------------|
| $\gamma$ | strain (-) |
|----------|------------|

|          |  |
|----------|--|
| $\delta$ | phase lag (rad)                          |
| $\eta$   | viscosity (Pa·s)                         |
| $\eta^*$ | complex viscosity (Pa·s)                 |
| $\sigma$ | stress (Pa)                              |
| $\omega$ | angular frequency (rad·s <sup>-1</sup> ) |

### *Abbreviations*

COP coefficient of performance

mPCM microencapsulated Phase Change Material

SEM scanning electron microscope

## **1. Introduction**

Over the last ten years a new technique had been proposed in the field of Thermal Energy Storage (TES) with Phase Change Materials (PCM). This new technique consists of forming a two-phase fluid from the mixture of a fluid such as water and a phase change material such as paraffin, resulting in a latent heat storage fluid generally called PCM slurry. There are different types of PCM slurries. Specifically, Inaba (2000) mentions five types of latent heat storage fluids: ice slurries, PCM microemulsions, microencapsulated PCM slurries, clathrate hydrate PCM slurries and shape-stabilized PCM slurries. This study concerns microencapsulated PCM slurries (mPCM slurries).

These new fluids offer many advantages and can be used either as thermal storage materials or heat transfer fluids (Royon and Guiffant, 2008) given that: 1) they have high storage capacity during phase change, 2) there is the possibility of using the same medium either to transport or store energy, as these slurries are pumpable (thus reducing heat transfer losses), 3) heat transfer occurs at an approximately constant temperature, 4) the heat transfer rate is high due to the elevated surface/volume ratio, 5) lower pumping power is required, as a consequence of the reduction in mass flow due to the higher heat capacity, 6) they provide a better cooling performance than conventional heat transfer fluids, due to the decrease in fluid temperature as a consequence of the higher heat capacity. Furthermore, these novel fluids have advantageous thermal energy storage densities compared to conventional systems of sensible heat storage in water and can be competitive against macroencapsulated PCM tanks. Besides, the response time may be shorter using these mPCM slurries as storage material than with macroencapsulated PCM. The tanks will be simpler as there is no need to macroencapsulate, and conventional tanks can be used.

These novel fluids can be used as heat transfer fluid and as thermal storage material in applications where water is used, and its heat capacity is a limiting factor. As an example, the following applications found in literature are described. The main application present in literature is the utilization of these PCM slurries as thermal storage materials and heat transfer fluids in chilled ceilings. Wang and Niu (2009) presented the results of a mathematical simulation of a combined system of chilled ceiling and storage tank with a mPCM slurry, in a room with the climatology of Hong Kong. The slurry was cooled and stored in the tank during the night, which resulted in electricity peak shaving, taking advantage of the nocturnal tariff and of a higher COP of the machine due to operation during lower environmental temperatures. During working hours, the mPCM slurry flowed from the tank to the chilled ceiling, melting the PCM and releasing the latent heat. Griffiths and Eames (2007) also studied the pumping of a mPCM slurry from BASF manufacturer with a 40% PCM concentration through a chilled ceiling in a room. The slurry was capable of maintaining a temperature of 20-21°C with a lower mass flow in comparison to water. Another well-known application, similar to the previously described, was carried out at the Narita Airport in Tokyo by Shibutani (2002). The issue in the installation of the Narita Airport in Tokyo was the change of refrigerants due to environmental reasons, without changing the chiller unit. This resulted in lower cooling power and the chiller was non-capable to absorb the demand peaks at specific times of the day. This problem was solved through the installation of a tank filled with a mPCM slurry custom-developed by Mitsubishi Heavy Industries. The cooling produced during the night by the chiller unit could be stored and reduce the demand peaks during the day. The slurry presented a storage density of 67 MJ/m<sup>3</sup>, higher in comparison to water, 21 MJ/m<sup>3</sup>. Vorbeck et al. (2013) tested a PCM slurry in a 5 m<sup>3</sup> storage tank pilot application, and they compared the results to water as reference medium. Depending on the operation temperature range the tested PCM slurry could store more than twice as much heat compared to water as conventional heat transfer fluid. Pollerberg and Dötsch (2006) proposed to use a dispersion of tetradecane with a 20% weight concentration for cooling supply networks. In this way, the required volumetric flow was lower, allowing for the reduction of the pumping power and pipe dimensions, with lower operation and investment costs. The increasing interest in PCM slurries as thermal storage material and as heat transfer fluid is proved in the review papers published recently (Zhang and Ma 2012, Delgado et al. 2012, Youssef et al. 2013).

Nevertheless, currently there is a lack of experience concerning its technical viability. Among the problems that mPCM slurries present that can influence their technical viability, the rupture of the microcapsules and stratification are the main issues to be tackled (Delgado et al. 2012).

Schalbart et al. (2010) analyzed the physical stability of different tetradecane nanoemulsions prepared by low-energy emulsification methods. All the samples stored at room temperature, without thickener, showed a

degree of creaming in two days. To prevent this phenomenon, the droplet size can be reduced (to nanometers) in order to increase homogeneity due to the Brownian motion. However, a lower droplet size increases the probability of subcooling (Günther et al. 2010). Another way to mitigate this unstabilization process is to employ thickeners, which would increase the viscosity and consequently would improve the stability. However, this higher viscosity would increase the pumping power in a real application. Stirring could be adopted in storage applications, however this may destroy the thermal stratification.

Huang et al. (2009) prepared and characterized several paraffin emulsions to propose an attractive candidate for cold storage and distribution problems. After a storage period of one month, they observed the creaming phenomenon in the samples containing 15-60 wt% paraffin, while no creaming was optically detected in the samples with 65-75 wt% paraffin.

Generally, these unstabilization processes in PCM slurries can take weeks, and even months. To predict the physical stability of PCM slurries and avoid waiting for complete unstabilization, a methodology well known in the food and pharmaceutical fields has been applied. This methodology basically consists of measuring the samples with a rheometer in oscillatory mode (Tadros 2004, Barnes 2000). These measurements can be related to those visually obtained during the unstabilization process of creaming. The dominant parameters in the unstabilization process are thus obtained, and these can be modified by manufacturers in order to improve the physical stability of PCM slurries. To complete the rheological analysis and characterization, the steady flow curves have also been obtained from rotational tests and the best fitting Viscosity-Shear rate model with these measurements is shown.

## **2. Materials and method**

### **2.1 Materials**

The analyzed mPCM slurry consists of microcapsules of paraffin coated with a polymer and dispersed in water through detergents, and it has been purchased in the commercial market. The mass fractions of the PCM microcapsules in the four mPCM slurries were 14, 20, 30 and 42% respectively, and the phase change temperatures range was approximately 21-24°C. The slurries with 14, 20 and 30% PCM microcapsule mass fractions were diluted from the slurry with 42% PCM microcapsules. These mass fractions are used in thermal storage applications. The particle size distribution was 2-20 µm according to the manufacturer's data, figure 1 shows an environmental SEM image, where the microscopic size can be detected. Figure 2 shows the Enthalpy-Temperature curves obtained with a T-history installation. When a material is being characterized, the sample must be representative of the material that is investigated. In this case, the PCM

slurry is constituted of different substances. The volume of the sample should be of at least a few cm<sup>3</sup> or more if possible, to assure that the sample has the correct chemical and physical composition that is representative of the bulk material (Lázaro et al. 2006). For this reason, an installation of the T-history method was chosen.

## 2.2 Methodology

For the physical stability analysis, a controlled stress rheometer was used, specifically a model AR-G2 rheometer supplied by TA Instruments. The minimum torque in oscillatory mode is 0.003  $\mu\text{N}\cdot\text{m}$  and in rotational mode 0.01  $\mu\text{N}\cdot\text{m}$ . They are not problematic values, since the samples have a considerable viscosity, and the torques applied are higher. To check if the rheometer measures appropriately, a reference substance has been measured, both in oscillatory mode and in rotational mode. This reference substance is the standard oil S60 from Canon Instruments Company (viscosity of 101 mPa·s at 25°C). The values of complex viscosity correspond to the values of dynamic viscosity (obtained in oscillatory mode), according to the Cox-Merz rule (Cox and Merz, 1958). In the flow curve, the average deviation to the reference values is 9.97%, and in the oscillatory curve, the average deviation is 6.50%. These tests have been carried out at 25°C, close temperature to the tests. Three repetitions of each test here presented were accomplished. No significant differences were observed.

There are two works in the literature, where the authors describe the measurement procedure to obtain Viscosity-Shear rate curves of PCM dispersions. In these studies they have used a cone as geometry (Huang et al. 2010, Royon et al. 1998). However in the work here presented a plate with a diameter of 40 mm was chosen, instead of a cone geometry, as a consequence of the size of the PCM microcapsules in suspension. According to the manufacturer's data, these PCM microcapsules have a diameter range from 2 to 20  $\mu\text{m}$ . In oscillatory tests, the particle size is not so important since the slurry does not flow due to the oscillatory motions of very low amplitude. Nevertheless, it is important in rotational tests where particles should flow without difficulty. The gap between plates or the gap of a truncated cone must be ten times greater than the particle size in suspension. The cone in our laboratory has a gap of 32  $\mu\text{m}$  and therefore it is not suitable for this slurry. In rotational tests using a plate, the shear rate is not constant over the whole radius of the geometry, so a correction (integrated in the software) must be applied.

To control the temperature of the sample, a Peltier plate was used together with a "solvent trap" accessory. With this accessory, a saturated atmosphere of humidity is created, avoiding the evaporation of the sample. The Peltier plate guarantees that the plate is at the set point temperature. If this set temperature is much higher or much lower than the room temperature, there might be temperature gradients on the sample. In

this case, the temperatures in the tests are closer to room temperature. Figure 3 shows the configuration used during the present tests.

### 2.2.1 Oscillatory tests

Oscillatory tests were carried out to analyze the rheological behavior of the mPCM. In this kind of test, the sample of the PCM slurry is subjected to a low amplitude oscillating strain and the stress to obtain this strain is measured. According to the phase lag between the applied strain ( $\gamma = \gamma_0 \cdot \cos(\omega t)$ ) and the measured stress ( $\sigma^* = \sigma_0 \cdot \cos(\omega t + \delta)$ ), if  $\delta=0^\circ$  the material is an elastic solid, if  $\delta=90^\circ$  it is a purely viscous fluid and if  $0 < \delta < 90^\circ$  it is a viscoelastic fluid. The elastic ( $G'$ ) and the viscous ( $G''$ ) modulus will be obtained in the following manner:

$$G' = \frac{\sigma^*}{\gamma} \cdot \cos \delta \quad (1)$$

$$G'' = \frac{\sigma^*}{\gamma} \cdot \sin \delta \quad (2)$$

Two kinds of tests were carried out: strain sweeps and frequency sweeps. In strain sweeps, the frequency is set, a strain or stress sweep is applied and the response is measured (stress or strain, respectively). In frequency sweeps, the strain or the stress is set, a frequency sweep is applied and the response is measured (stress or strain). These kinds of tests provide information about the stability of the structural network of the mPCM slurry.

The frequency sweeps covered a frequency range from 0.005 Hz to 100 Hz. These were accomplished within the linear viscoelastic region. To test within this region, previously the strain sweeps were executed from 0.01 to 10 at 1 Hz. Although the permanence within the linear viscoelastic region must also be guaranteed above 1 Hz, this value of frequency was considered sufficient since above 1 Hz measurements showed much inertia (the relation between inertia and frequency is quadratic). The oscillating motion of the axle experiences a delay introduced by the inertia of the motor and by the inertia of the geometry. In oscillatory tests, inertia can be relevant since a phase lag between the sinusoidal wave applied and the responding sinusoidal wave is introduced. Obviously, this phase lag must be known in order to eliminate it. The software calculates this value for its correction from the inertia of the motor and of the geometry. In spite of this correction, it is advisable not to take into account measurements at high frequencies. Furthermore, the analysis of interest is at low frequencies for the study of physical stability during storage or rest.

Structured fluids usually present a similar qualitative global behavior when a frequency sweep is carried out. From  $G'$ - $\omega$  and  $G''$ - $\omega$  curves, information about the microstructure of the PCM slurry in qualitative terms can be obtained. In fact, the  $G'$  value at the frequency where  $G''$  presents a minimum is related to the structural stability of the dispersed system. Higher  $G'$  values mean greater stability (Tadros 2004). These values measured by the rheometer can be related to the destabilization processes observed in the mPCM slurries, specifically with the creaming process which causes stratification problems. For this purpose, calibrated test tubes were filled with four PCM slurries (14, 20, 30 and 42% mass fraction of PCM microcapsules) and the temporal evolution of the creamed height was observed.

### **2.2.2 Rotational tests**

Flow tests or rotational tests consist of applying a torque (or stress) and measuring the strain, to obtain viscosity values. Shear rate sweeps from  $0.001$  to  $1000\text{ s}^{-1}$  were carried out to obtain the viscosity-shear rate curves. For this purpose, a stress is applied on the sample. This stress is controlled by the rheometer, and changed in the course of the test to complete the shear rate sweep. The measurement of the viscosity is accomplished when the material has reached the steady flow state. The stress is increased logarithmically and the process is repeated, providing the steady flow viscosity curve. For the definition of the steady state, it has been proposed as a condition that the variation of the stress for three consecutive points should be lower than 5%. When this condition is achieved, it is considered that the steady state has been reached and the last viscosity value is taken as a valid measurement.

## **3. Results and discussion**

### **3.1 Previous results**

Before obtaining viscosity measurements, a time sweep was carried out to study the possible evaporation of the sample, and to determine in this manner the maximum duration of the tests. In this test, the elastic and viscous component of the slurry over time is measured (for a set frequency and a set strain). The evaporation of the solvent means an increase in these two components. Water loss would result in the behavior of the slurry tending towards the behavior of a solid and it would be more viscous because of the higher PCM concentration.

Figure 4 shows the results of a time sweep on the mPCM slurry with 42% PCM microcapsules mass fraction without the use of the solvent trap. As slurries are complex fluids, a pre-shear of  $100\text{ s}^{-1}$  during one minute was done to break completely the structure of the sample (during the load of the sample with a pipette, the structure was partially broken). The sample needed about 600 seconds to recover its structure and from

1200 seconds it started to evaporate. This time (1200-600=600 seconds) was insufficient to carry out a test. When the plate was lifted up, drying of the sample was observed. The visual results and the results obtained with the rheometer were matched, since the elastic and the viscous module had increased. When the solvent trap was used and a balancing time was given for the restructuring of the sample (determined for the previous test), the graph in figure 5 was obtained. During an hour, the elastic and viscous module remained constant, and therefore drying of the sample did not take place.

### 3.2 Results of the oscillatory tests

Firstly, a strain sweep at 1 Hz was accomplished to determine the linear viscoelastic region. This is the region where the relation between stress/strain of a viscoelastic material is linear. Figure 6 shows the results obtained for the four mPCM slurries. The sample is no longer within the linear viscoelastic region when the  $G'$  modulus falls quickly. Once this region was determined, a strain value within this linear viscoelastic region was chosen, and the frequency sweep was carried out. Although the values obtained at high frequencies were very different (maybe the consequence of a higher inertia), these results are not really important. The interest lies in the  $G'$  and  $G''$  modulus at low frequencies (long time period, at rest), since it is the structural stability of these slurries at rest in a tank that is to be studied.

The most extensive  $G'$  and  $G''$  moduli of real examples of structured liquids are shown in figure 7. The exact values of the  $G'$  and  $G''$  moduli and their position in the frequencies scope will change, but their qualitative overall behavior will be as shown in the figure, provided that such a wide frequency range can be determined. The rheometers usually work within the range from 0.01 to 100  $\text{rad}\cdot\text{s}^{-1}$  and they just can see two of the zones described in the figure.

If the frequency sweeps are compared (figure 8) to the typical oscillatory response of structured fluids (figure 7), it is observed that the test covers the “plateau” and “transition” zones only. The “rubbery” or “plateau” zone is the region where elastic behavior is more predominant. Whereas there is a plateau in many cases, in fact there is always a slight increase in the  $G'$  modulus with the frequency. The  $G''$  modulus is always lower than the  $G'$  modulus, but it can sometimes be significant. When the slope of  $G'-\omega$  is low, the  $G''$  value decreases when increasing  $\omega$  up to a minimum where it rises again. The lower the slope of the  $G'-\omega$  curve, the deeper is the valley of  $G''$  (Barnes 2000).

It is observed that at very low frequencies, the  $G'$  modulus remains constant. However, a minimum in the  $G''-\omega$  curve is not observed so clearly, only for the slurry with a 42% PCM microcapsule mass fraction. From these  $G'-\omega$  and  $G''-\omega$  curves, information in qualitative terms about the microstructure of the slurry can be obtained. In fact, the  $G'$  value for the frequency  $\omega$  where  $G''$  shows a minimum (“plateau” zone) is related to

the structural stability of the system. With higher  $G'$  values, the stability improves. The minimum of the  $G''-\omega$  curves is not observed clearly, maybe because it is located at lower  $\omega$  values than the tested  $\omega$  values. As  $G'$  remains constant, this value has been taken for the other three curves. Also the value of  $\tan \delta = G''/G'$  has been taken, which also gives information about stability. These values are collected in table 1. From this frequency sweep, the fact of that the  $G'$  and the  $G''$  module for the slurry with 20% PCM microcapsules in comparison to 30% PCM microcapsule is higher, attracts the attention. Different samples were analyzed, not obtaining significant differences. This phenomenon will be studied in subsequent studies.

It is observed that at low frequencies the values of  $\tan \delta$  are low, about 0.25. This means that the elastic part of the slurry is much greater than the viscous part (as observed in figure 8), i.e. interaction between the particles that form the slurry is very strong. These forces between particles will promote their aggregation and are able to cause phenomena of flocculation or coalescence.

We attempted to relate the values measured by the rheometer with the unstabilization processes observed in the mPCM slurries, specifically with the creaming process. In a highly stable system, where Brownian motion is negligible for the micron sized particle, the action of gravity causes the PCM particles with a lower density than water to move upward, causing a rise in the PCM microcapsule concentration in the upper part. An increase in the average rapprochement between the particles is thus caused to such an extent that attractive forces predominate. The creaming caused in this manner is a creaming of low volume. The small particles occupy the cavities that the bigger particles leave, forming a compact packaging. These kinds of slurries are called deflocculated slurries and they are characterized by a long creaming time, a small volume of creaming and a muddy aspect of the water. It is difficult to re-disperse the particles in suspension. On the other hand, there are slurries where the stability is insufficient, and the aggregation of particle groups or floccules occurs before creaming. The creaming volume is greater, the creaming time is shorter, the water is clear and it is easy to re-disperse the slurry. These kinds of slurries are called flocculated slurries (Gerbino 2011).

The sedimentation rate of very diluted slurries of rigid and spherical particles without interaction follows the Stokes law. However, the sedimentation or creaming of more concentrated slurries is a more complex process.

The relationship between the observed creaming phenomenon and the measured rheological parameters was evaluated and established as follows. Four calibrated and graduated test tubes with a volume of 10 ml were prepared and the height or volume of the creaming part over time was observed, from the graduation of the tubes. These test tubes have been verified according to the ISO Standard 4788:2005. The average volume at 20°C is 10.016 ml, with a standard error of 0.021 ml. During the first days, the measurements were

taken every 30 minutes. After these first days, the interval of data gathering was every 24 hours. Figure 9 shows the test tubes on the seventh day and figure 10 shows the creaming percentage over time.

The creaming percentage has been calculated using equation 3:

$$\text{Creaming}(\%) = \frac{V_{\text{water, lower part}}}{V_{\text{total water slurry}}} \cdot 100 \quad (3)$$

Figure 11 shows the creaming percentage for a time  $t=31703$  minutes against the  $G'$  modulus, according to the stability criterion explained above. It is observed that a higher  $G'$  modulus means a lower creaming percentage for a given time. In other words, the slurry is more stable during a longer time when the  $G'$  modulus is high. On the other hand, if attention is paid to the values of  $\tan \delta$  shown in table 1, it is observed that the four slurries show a very low  $\tan \delta$ . This means that the elasticity level is too high and the forces between particles cause aggregation and flocculation.

From the strain sweeps, the stability of these slurries can also be evaluated. In the strain sweeps at 1 Hz, the values of critical strain and the  $G'$  modulus have been obtained. From these values, the cohesive energy of the flocculated structure can be calculated according to equation 4. These values are gathered together in table 2. Figure 12 shows this cohesive energy against the creaming percentage for a time  $t=31703$  minutes. Obviously, the higher the cohesive energy or attraction between particles and floccules, the higher the flocculation level of the structure, and therefore the creaming percentage is greater since larger floccules are formed.

$$E_c = \int_0^{\gamma_{cr}} \sigma \cdot d\gamma = \int_0^{\gamma_{cr}} G' \cdot \gamma \cdot d\gamma = \frac{1}{2} G' \cdot \gamma_{cr}^2 \quad (4)$$

The values shown in table 2 were obtained from the strain sweeps. A comparison between the results obtained and those observed shows that they are consistent. In the case of the slurry with a 42% PCM microcapsule mass fraction, which has lower cohesive energy or attraction energy, the results match with the longer creaming time typical of less flocculated or deflocculated slurries. On the other hand, in the case of the slurry with a 14% PCM microcapsule mass fraction, which has higher cohesive energy or attraction between floccules, there is a much faster creaming process typical of strongly flocculated slurries.

### 3.3 Results of the rotational tests

Once the oscillatory tests were accomplished, a rotational test was carried out at a temperature of 27°C for the four mPCM slurries (14, 20, 30 and 42% PCM microcapsule mass fractions), obtaining the flow curves shown in figure 13. The software tool “Best fit Viscosity-Shear rate” was used.

It is observed that when the shear rate rises, the viscosity decreases and then reaches a Newtonian plateau where it remains constant. This shear-thinning behavior is found in some works of literature (Huang et al. 2010, Royon et al. 1998, Lu and Tassou 2012, Chen et al. 2008). There are also other works where a Newtonian behavior has been shown when working with PCM concentrations lower than 25% (Wang et al. 2007, Zhang and Zhao 2011). This shear-thinning phenomenon can be explained by the spatial distribution of the microcapsules in suspension. When a slurry is stable and at rest, particles are arranged in a random way in the continuous phase. When the slurry is sheared at very low shear rates, there is no cooperative motion between the microcapsules so that they move in the flow direction, and therefore the viscosity is high. However, when the slurry is sheared at high velocities, the microcapsules start to move from their random distribution towards a situation where layers are formed. In this way, the average distance between particles decreases in the flow direction and increases in the perpendicular direction. This change in spatial distribution facilitates the movement of the particles and the viscosity drops.

The Newtonian plateau is reached at shear rates about 10-100 s<sup>-1</sup>. A flowing fluid would have shear rates within the range of the Newtonian plateau. According to the software tool “Best fit Viscosity-Shear”, the model that gives the best fitting for the four mPCM slurries is the Carreau model (Carreau 1972). Equation 5 shows this model and table 3 shows the adjustment coefficients:

$$\frac{\eta - \eta_\infty}{\eta_0 - \eta_\infty} = \frac{1}{(1 + (k \cdot \dot{\gamma})^2)^{m/2}} \quad (5)$$

Comparing the four flow curves, those for the slurries with mass fractions of 14%, 20%, 30% and 42% the viscosity is multiplied by a factor five, six, eighteen and eighty compared to water respectively. Both the curve flow for the slurry with a 14% PCM microcapsule mass fraction and for the slurry with a 20% PCM microcapsule mass fraction show a rise in the viscosity above 200 s<sup>-1</sup>. This phenomenon is not very common in slurries. Tests have shown that liquids of low viscosity at very high shear rates can cause secondary flows, increasing the apparent viscosity (Barnes 2000).

#### 4. Conclusions

The physical stability of four mPCM slurries with different PCM microcapsule mass fractions has been studied using a control stress rheometer. For this purpose, oscillatory tests have been accomplished. Different stability criteria found in the literature have been applied and related to the unstabilization process observed in the samples, in this case related to the creaming process. From the frequency sweeps accomplished, an exponential relationship between the creaming percentage and the elastic module of the mPCM slurries have been obtained. From the strain sweeps, the cohesive energies of the mPCM slurries

have been calculated and related to the creaming percentage, obtaining a linear relationship. From the relationships established, these correlations could be used as a guide for manufacturers to reformulate mPCM slurries and achieve better physical stability. The duration of the unstabilization time could be estimated without having to wait until the complete unstabilization process is completed.

Another potential use of the methodology presented to study the physical stability of PCM slurries could be the investigation of thickening agents to avoid the incongruent melting of inorganic PCMs, since testing in this case also is a time consuming process.

In addition, the behavior models that describe the flow curve have been obtained. A shear-thinning behavior has been observed and the Viscosity-Shear rate values of the curves obtained have been fitted to the Carreau model.

## 5. References

Barnes, H.A., 2000. A handbook of elementary rheology, Institute of Non-Newtonian Fluid Mechanics, University of Wales.

Carreau, J.P., 1972. Rheological Equations from Molecular Network Theories. *Trans. Soc. Rheol.* 16, 99-127.

Chen, B., Wang, X., Zeng, R., Zhang, Y., Wang, X., Niu, J., Li, Y., Di, H., 2008. An experimental study of convective heat transfer with microencapsulated phase change material suspension: Laminar flow in a circular tube under constant heat flux. *Exp. Therm. Fluid Sci.* 32, 1638-1646.

Cox, W.P., Merz, E.H., 1958. Correlation of dynamic and steady flow viscosities. *J. Polym. Sci.* 28, 619-622.

Delgado, M., Lázaro, A., Mazo, J., Zalba, B., 2012. Review on phase change material emulsions and microencapsulated phase change material slurries: Materials, heat transfer studies and applications. *Renew. Sustain. Energy Rev.* 16, 253-273.

Gerbino, P.P., 2011. The Science and Practice of Pharmacy, 21<sup>st</sup> Edition, Philadelphia, PA. Lippincott Williams & Wilkins.

Griffiths, P.W., Eames, P.C., 2007. Performance of chilled ceiling panels using phase change material slurries as the heat transport medium. *Appl. Therm. Eng.* 27, 1756-1760.

Günther, E., Schmid, T., Mehling, H., Hiebler, S., Huang, L., 2010. Subcooling in hexadecane emulsions. *Int. J. Refrig.* 33, 1605-1611.

Huang, L., Petermann, M., Doetsch, C., 2009. Evaluation of paraffin / water emulsion as a phase change slurry for cooling applications. *Energy*. 34, 1145-1155.

Huang, L., Doetsch, C., Pollerberg, C., 2010. Low temperature paraffin phase change emulsions. *Int. J. Refrig.* 33, 1583-1589.

Inaba, H., 2000. New challenge in advanced thermal energy transportation using functionally thermal fluids. *Int. J. Therm. Sci.* 39, 991-1003.

Lázaro, A., Günther, E., Mehling, H., Hiebler, S., Marín, J.M., Zalba, B., 2006. Verification of a T-history installation to measure enthalpy versus temperature curves of phase change materials. *Meas. Sci. Tecnol.* 17, 2168-2174.

Lu, W., Tassou, S.A., 2012. Experimental study of the thermal characteristics of phase change slurries for active cooling. *Appl. Energy* 91, 366-374.

Pollerberg, C., Dötsch, C., 2006. Phase Changing Slurries in cooling and cold supply networks. 10<sup>th</sup> International Symposium on District Heating and Cooling, Hannover (Germany).

Ryon, L., Perrot, P., Guiffant, G., Fraoua, S., 1998. Physical properties and thermorheological behaviour of a dispersion having cold latent heat-storage material. *Energy Convers. Manag.* 39, 1529-1535.

Ryon, L., Guiffant, G., 2008. Forced convection heat transfer with slurry of phase change material in circular ducts: A phenomenological approach. *Energy Convers. Manag.* 49, 928-932.

Schalbart, P., Kawaji, M., Fumoto, K., 2010. Formation of tetradecane nanoemulsion by low-energy emulsification methods. *Int. J. Refrig.* 33, 1612-1624.

Shibutani, S., 2002. PCM-microcapsule slurry thermal storage system for cooling in Narita Airport. Proc. Of the 3<sup>rd</sup> Experts meeting and Workshop of IEA Annex 17, Tokyo (Japan).

Tadros, T., 2004. Applications of rheology for assessment and prediction of the long-term physical stability of emulsions. *Adv. Colloid Interface Sci.* 108-109, 227-258.

Vorbeck, L., Gschwander, S., Thiel, P., Lüdemann, B., Schossig, P., 2012. Pilot application of phase change slurry in a 5 m<sup>3</sup> storage. *Appl. Energy*, In Press, Corrected Proof.

Wang, X., Niu, J., Li, Y., Wang, X., Chen, B., Zeng, R., Song, Q., Zhang, Y., 2007. Flow and heat transfer behaviors of phase change material slurries in a horizontal circular tube. *Int. J. Heat Mass Transf.* 50, 2480-

Wang, X., Niu, J., 2009. Performance of cooled-ceiling operating with MPCM slurry. *Energy Convers. Manag.* 50, 583-591.

Youssef, Z., Delahaye, A., Huang, L., Trinquet, F., Fournaison, L., Pollerberg, C., Doetsch, C., 2013. State of the art on phase change material slurries. *Energy Convers. Manag.* 65, 120-132.

Zhang, G.H., Zhao, C.Y., 2011. Thermal and rheological properties of microencapsulated phase change materials. *Renew. Energy* 36, 2959-2966.

Zhang, P., Ma, Z.W., 2012. An overview of fundamental studies and applications of phase change material slurries to secondary loop refrigeration and air conditioning systems. *Renew. Sustain. Energy Rev.* 16, 5021-5058.

<http://www.tainstruments.com/> (access in April 2013)

## 6. Acknowledgements

The authors would like to thank the Spanish government for partially funding this work within the framework of research projects (MICINN-FEDER): ENE2008-06687-C02/CON and ENE2011-28269-C03-01. The authors would also like to thank the CIAT company for its participation and support within the framework of the SOLTES project, partially funded by the Innovation and Development Agency of Andalucía (IDEA) and by the Industrial Technological Development Centre (CDTI). Mónica Delgado is especially grateful to the Vice Deanship for Research of the University of Zaragoza for her grant.

## Figures and tables captions

Figure 1. Environmental SEM image of the mPCM slurry.

Figure 2. Enthalpy-Temperature curves obtained with a T-history installation for mPCM slurries with different mass fractions.

Figure 3. Configuration of the rheometer employed in the experiments (TA Instruments)

Figure 4. Time sweep without solvent trap. mPCM slurry with 42% PCM microcapsules. Temperature=27°C, strain=0.1, frequency=1 Hz. Sample loaded with pipette and pre-shear.

Figure 5. Time sweep with solvent trap after pre-shear and balancing time. mPCM slurry with 42% PCM microcapsules. Temperature=27°C, strain=0.1, frequency=1 Hz.

Figure 6. Strain sweep for the four PCM microcapsule mass fractions, temperature=27°C, frequency=1 Hz.

Figure 7. Oscillatory response for real systems (Barnes 2000).

Figure 8. Frequency sweeps according to the PCM microcapsule mass fraction. Temperature=27°C, strain=0.1

Figure 9. Creaming observed at t=10080 minutes.

Figure 10. Creaming percentage over time.

Figure 11. Relationship between the G' modulus and the creaming at t=31703 minutes.

Figure 12. Relationship between the Cohesive Energy and Creaming percentage.

Figure 13. Viscosity-shear rate curves according to the PCM microcapsule mass fraction.

Table 1. Values obtained from the frequency sweeps for the study of the structural stability of PCM slurries

Table 2. Values obtained from the strain sweep for the study of the structural stability of PCM slurries

Table 3. Parameters according to the Carreau model (Carreau 1972).

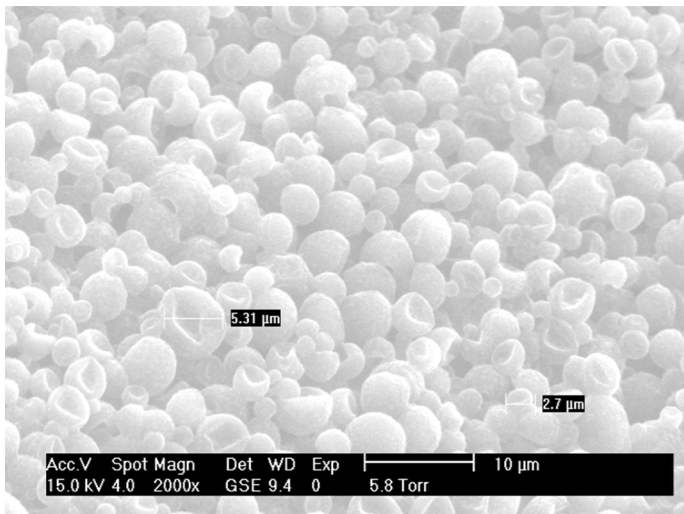


Figure 1.

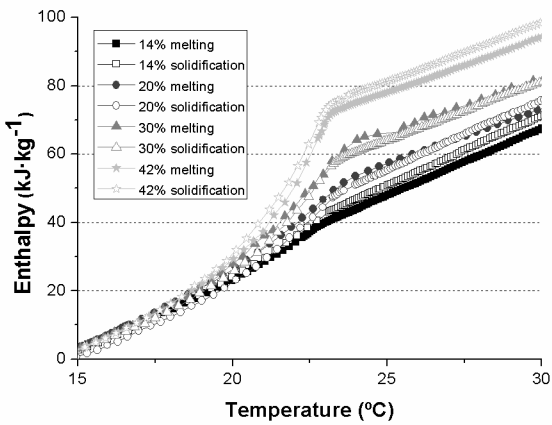


Figure 2.

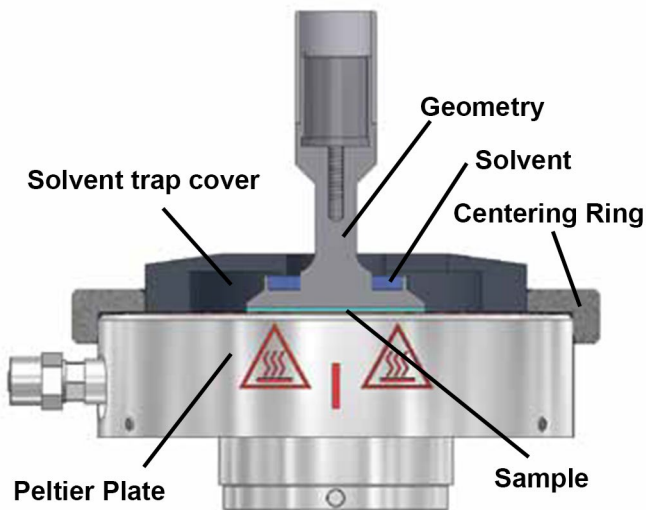


Figure 3.

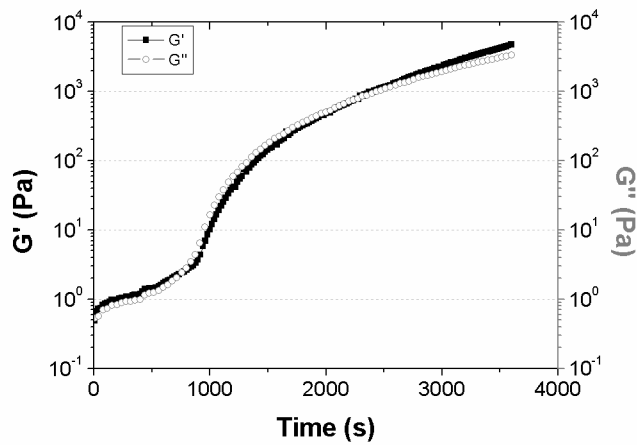


Figure 4.

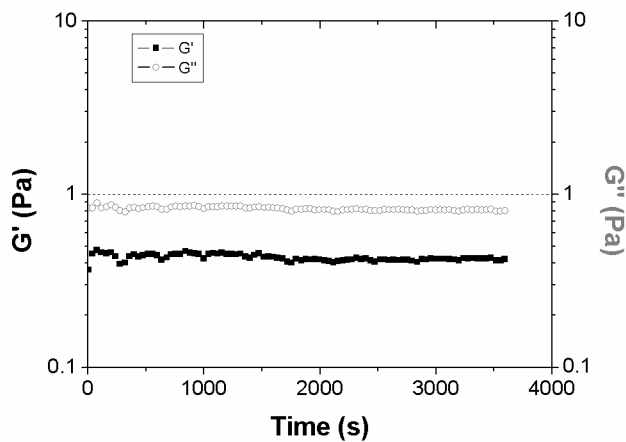


Figure 5.

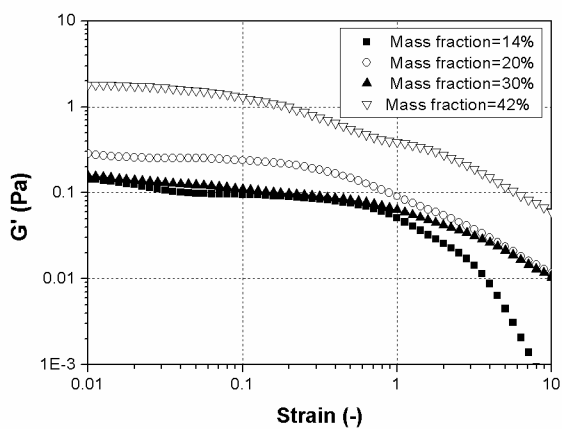


Figure 6.

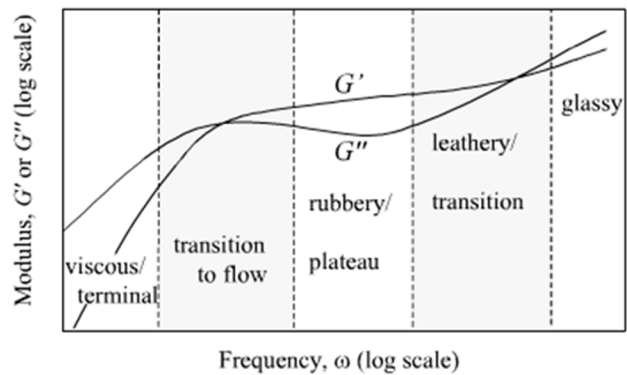


Figure 7.

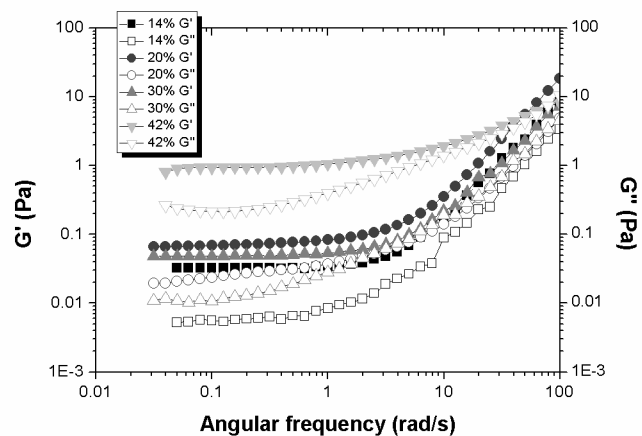


Figure 8.

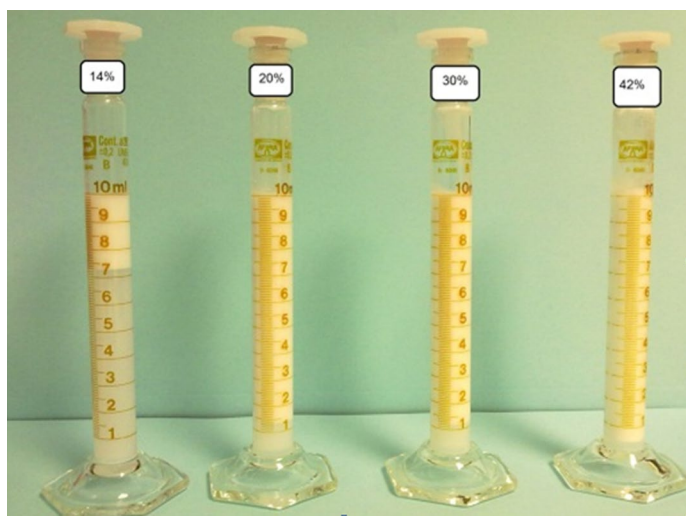


Figure 9.

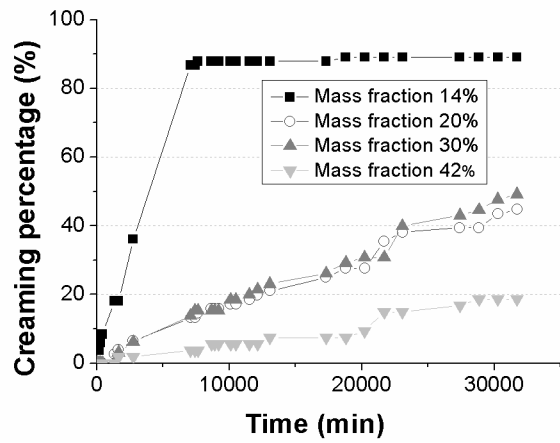


Figure 10.

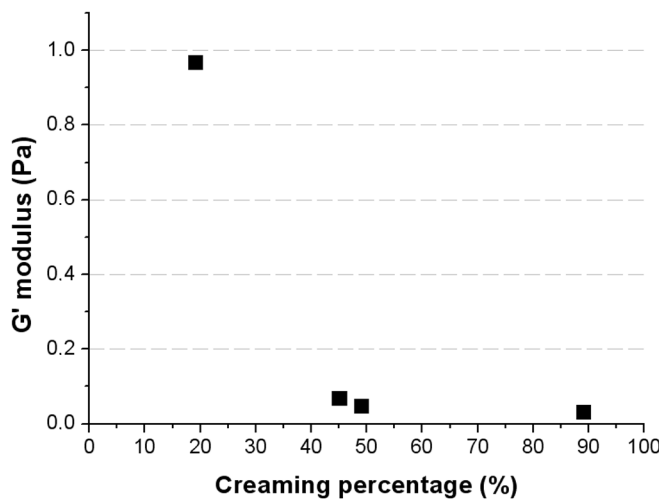


Figure 11.

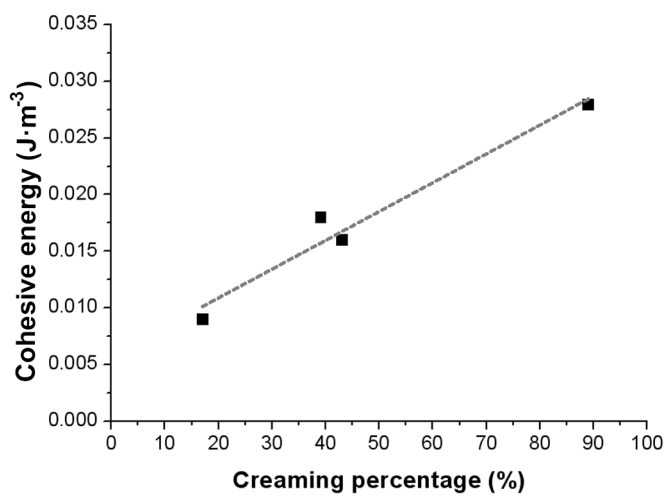


Figure 12.

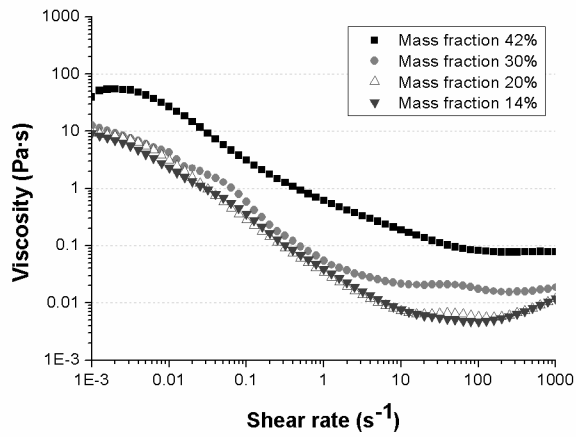


Figure 13.

| PCM microcapsules concentration | G' modulus | $\tan\delta$ |
|---------------------------------|------------|--------------|
| 14%                             | 0.032      | 0.1785       |
| 20%                             | 0.070      | 0.3461       |
| 30%                             | 0.048      | 0.2322       |
| 42%                             | 0.968      | 0.2438       |

Table 1.

| PCM microcapsules concentration | G' modulus (f=1Hz) | Critical strain (-) | Cohesive energy (J·m⁻³) |
|---------------------------------|--------------------|---------------------|-------------------------|
| 14%                             | 0.09               | 0.79                | 0.028                   |
| 20%                             | 0.24               | 0.39                | 0.030                   |
| 30%                             | 0.13               | 0.50                | 0.016                   |
| 42%                             | 1.80               | 0.10                | 0.009                   |

Table 2.

| PCM microcapsules concentration | $\eta_0$ (Pa·s) | $\eta_\infty$ (Pa·s)  | k (s)  | m    | Standard error |
|---------------------------------|-----------------|-----------------------|--------|------|----------------|
| 14%                             | 13.80           | $4.89 \cdot 10^{-3}$  | 288.80 | 1.02 | 18.36          |
| 20%                             | 10.88           | $6.45 \cdot 10^{-3}$  | 315.40 | 1.06 | 17.11          |
| 30%                             | 6.45            | $18.32 \cdot 10^{-3}$ | 82.05  | 1.03 | 17.70          |
| 42%                             | 41.07           | $7.520 \cdot 10^{-2}$ | 237.00 | 0.77 | 19.00          |

Table 3.